

## Indolin-2-one p38 $\alpha$ inhibitors I: Design, profiling and crystallographic binding mode

Paul Eastwood\*, Jacob González, Elena Gómez, Bernat Vidal, Francisco Caturla, Ramón Roca, Cristina Balagué, Adelina Orellana, María Domínguez

Almirall Research Center, Almirall S.A., Ctra. Laureà Miró 408, E-08980 St. Feliu de Llobregat, Barcelona, Spain

### ARTICLE INFO

#### Article history:

Received 26 April 2011

Revised 25 May 2011

Accepted 28 May 2011

Available online 6 June 2011

#### Keywords:

p38 $\alpha$  Inhibitors

Structure-based design

Molecular modeling

Indolin-2-ones

X-ray crystallography

### ABSTRACT

The use of structure-based design and molecular modeling led to the discovery of indolin-2-one derivatives as potent and selective p38 $\alpha$  inhibitors. The predicted binding mode was confirmed by X-ray crystallography.

© 2011 Elsevier Ltd. All rights reserved.

The p38 $\alpha$  mitogen activated protein (MAP) kinase is an intracellular serine/threonine (Ser/Thr) kinase that is activated by a range of environmental stimuli such as TNF $\alpha$ , IL-1 $\beta$  and stress.<sup>1,2</sup> Activation of p38 $\alpha$  occurs through bisphosphorylation by the dual-specificity Ser/Thr MAP kinases MKK3 and MKK6 on the Thr180-Gly181-Tyr182 motif located on the activation loop.<sup>2,3</sup> In the activated state, p38 $\alpha$  phosphorylates a range of intracellular protein substrates that post-transcriptionally regulate the biosynthesis of the cytokines TNF $\alpha$  and IL-1 $\beta$ . The pathophysiological consequence of excessive production of TNF $\alpha$  and IL-1 $\beta$  is thought to be significant in the progression of many inflammatory diseases such as rheumatoid arthritis, psoriasis and inflammatory bowel disease.<sup>4–7</sup> The inhibition of p38 $\alpha$  MAP kinase can efficiently regulate both the release and the activity of such pro-inflammatory cytokines and has thus been seen as an opportunity to discover novel anti-inflammatory drugs.<sup>8</sup>

Since the first report in 1994 of the pyridylimidazole-based p38 $\alpha$  inhibitor SB203580,<sup>9</sup> a variety of compounds advanced into clinical trials.<sup>10</sup> The robust preclinical validation of the target along with the reported efficacy for VX-745<sup>11,12</sup> spurred the conceptualization of novel p38 $\alpha$  MAPK inhibitors with improved pharmacological profiles. However, recent clinical results obtained for the most advanced compounds in rheumatoid arthritis have unveiled only a transient reduction in inflammation which may have compromised overall efficacy.<sup>13</sup> The use of p38 $\alpha$  inhibitors in other indications is currently under evaluation.

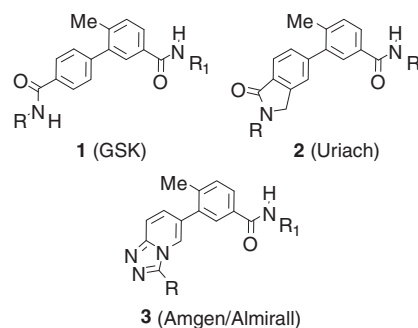


**Figure 1.** Representative examples of reported 'biaryl amide'-type p38 $\alpha$  inhibitors.

Several series of p38 $\alpha$  inhibitors containing a biaryl-amide moiety have been reported<sup>14,15</sup>—a selection of representative examples are shown in Figure 1.

A number of co-crystal structures of compounds of type **1** bound in p38 $\alpha$  have been solved<sup>15a</sup> and the key hydrogen-bonding interactions are as shown in Figure 2. One of the amide moieties forms two key hydrogen-bonding interactions with Asp168 and Glu71, a feature which is typical of other tolylamide p38 $\alpha$  inhibitors.<sup>16</sup> The carbonyl group of the distal amide forms a hydrogen bond with Met109 of the hinge region, the residue which forms a key interaction with the vast majority of p38 $\alpha$  inhibitors. Depending on the particular substitution pattern in **1**, an additional interaction may be seen in the hinge region between the same

\* Corresponding author.

E-mail address: [paul.eastwood@almirall.com](mailto:paul.eastwood@almirall.com) (P. Eastwood).

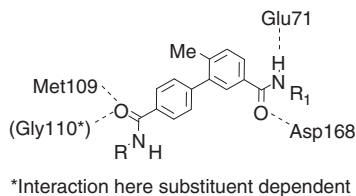


**Figure 2.** Key hydrogen-bonding interactions between structures of type **1** and p38 $\alpha$ .

carbonyl group and the NH of Gly110. The latter interaction is achieved via a 'flip' of this particular amino acid in which the NH of the residue is orientated towards the interior of the binding pocket and the carbonyl group to the exterior, the reverse orientation to that seen in the apo protein and many other p38 $\alpha$  X-ray crystal structures with bound ligands. The corresponding hinge residues in closely related kinases bear larger side chains preventing facile amide bond re-orientation. Thus, in addition to having an additional hydrogen-bonding interaction, compounds which bind in the 'flip' mode may be more selective with respect to other kinases.<sup>17</sup>

In-house modeling studies (see Fig. 3) suggested that the hydrogen-bonding interaction with Gly110 could be favored further by increasing the distance between the interacting carbonyl group and the aromatic moiety if all other interactions remained the same (structure **4**). To fix the position and orientation of the carbonyl group in **4** we considered various cyclic derivatives, one option being indolin-2-ones of general structure **5**. Bis-alkylation at the benzylic position forming a gem-dialkyl or spirocyclic group would allow occupancy of the hydrophobic pocket in this region of the enzyme and prevent oxidative metabolism at this centre. Mono alkylation was not considered as a potentially racemizable chiral centre would be formed. Herein it is reported that compounds of type **5** are potent and selective p38 $\alpha$  inhibitors.

Synthetic routes to compounds are given in Schemes 1–3. Key indolin-2-one intermediates of type **7** were synthesized by one of two routes. The first route involved the double alkylation of the oxindole intermediate **6** to form the spiranic ring system.<sup>18</sup> The second route (Scheme 2) involved treatment of hydrazide derivatives **10** with a calcium base at high temperatures giving rise to separable mixtures of regioisomers.<sup>19</sup> Indolin-2-one intermediates **7–9** were then cross-coupled under palladium catalysis with suitably functionalized derivatives **11** to give biaryls **12** followed by amide bond formation to give the desired final products (Scheme 3). Alternatively the final products could be accessed in one step by cross-coupling with an appropriate amide derivative **13**.

Biological results are presented in Table 1.<sup>20</sup> The cyclopropyl amide has proven to be one of the optimal amide substituents in other published 'biaryl amide' series and was thus installed in the first compounds synthesized. It can be seen from the results

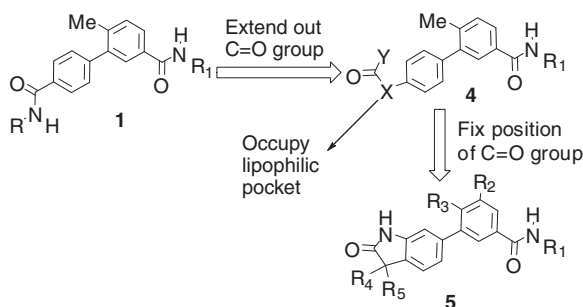
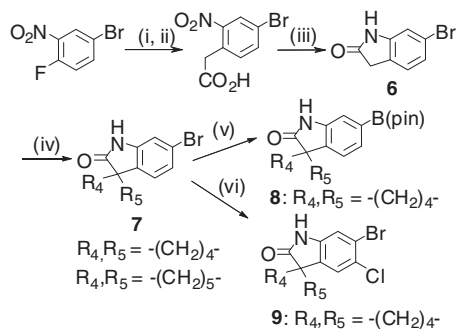
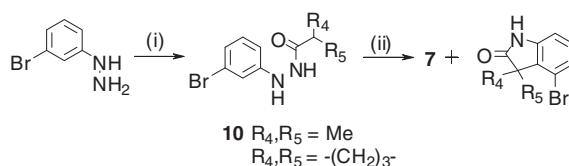


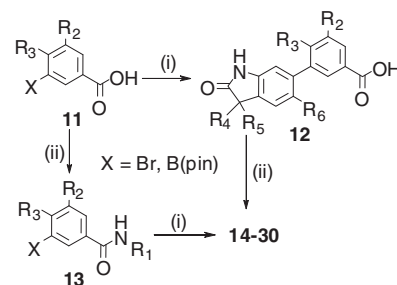
**Figure 3.** Design of indolin-2-one p38 $\alpha$  inhibitors **5**.



**Scheme 1.** Reagents and conditions: (i) NaH, dimethylmalonate, DMF, 0–65 °C, 83%; (ii) 6 M HCl (aq), DMSO, 130 °C, 94%; (iii) Fe, AcOH, 75–100 °C, 61%; (iv) BuLi, TMEDA, I(CH<sub>2</sub>)<sub>n</sub>I (n = 4 or 5), THF, –78 °C to rt, 24–45%; (v) bis(pinacolato)diboron, KOAc, PdCl<sub>2</sub>dppf·CH<sub>2</sub>Cl<sub>2</sub>, DMF, 120 °C, microwave, 30–50%; (vi) NCS, CHCl<sub>3</sub>, reflux, 75%.



**Scheme 2.** Reagents and conditions: (i) acid chloride, Et<sub>3</sub>N, DCM, rt, 60–78%; (ii) R<sub>4</sub>, R<sub>5</sub> = Me, CaH<sub>2</sub>, 180–230 °C, 24%; R<sub>4</sub>, R<sub>5</sub> = -(CH<sub>2</sub>)<sub>3</sub>–, CaO, quinoline, 265 °C, 17%.



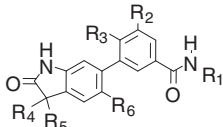
**Scheme 3.** Reagents and conditions: (i) compound **7**, **8** or **9**, PdCl<sub>2</sub>dppf·CH<sub>2</sub>Cl<sub>2</sub>, 2 M Cs<sub>2</sub>CO<sub>3</sub> (aq), dioxane, 90–100 °C; (ii) R<sub>1</sub>NH<sub>2</sub>, HATU, DIPEA, DMF, rt.

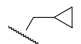
obtained with compounds **14–18** that indolin-2-ones of general structure **5** are potent p38 $\alpha$  inhibitors. In general, a 3- to 10-fold loss of potency was observed in going from the enzymatic assay to the human whole blood assay although inexplicable differences in potency between similar compounds often arose in these two assays. For example, compounds **15** and **16**, which have the same enzymatic potency, and are not likely to differ significantly with respect to physicochemical properties, show almost an order of magnitude of difference in the whole blood assay.

With respect to the SAR at R<sub>3</sub>, replacement of the methyl by a chlorine substituent (compd **18**) gave essentially an equipotent derivative. However, the placement of hydrogen at this position (compd **19**) results in the loss of two orders of magnitude of potency. A small substituent in this position probably fulfills the dual function of filling the small lipophilic pocket in this region (vide infra) and contributes to a favorable twist arrangement of the two aromatic rings necessary for optimal binding. Indeed, maintaining this hydrogen at R<sub>3</sub> whilst placing a Cl atom at R<sub>6</sub> in the adjacent aromatic ring (compd **20**) favours the twist arrangement and somewhat restores enzymatic potency (although whole blood potency suffers in this particular case).

Fixing the indolin-2-one substituent as a five-membered spiranic ring, it can be seen that the optimal substituents for the amide

**Table 1**  
Structures and biological activities of indolin-2-one derivatives<sup>20</sup>



Compd	R <sub>1</sub>	R <sub>2</sub>	R <sub>3</sub>	R <sub>4</sub> , R <sub>5</sub>	R <sub>6</sub>	p38α IC <sub>50</sub> <sup>a</sup> (nM)	Whole blood IC <sub>50</sub> <sup>a</sup> (nM)
SB203580	—	—	—	—	—	55 ± 10	190 ± 7
<b>14</b>	Cyclopropyl	H	Me	Me, Me	H	5 ± 2	15.5 ± 2
<b>15</b>	Cyclopropyl	H	Me	-(CH <sub>2</sub> ) <sub>3</sub> -	H	1.4 ± 0.3	123 ± 9
<b>16</b>	Cyclopropyl	H	Me	-(CH <sub>2</sub> ) <sub>4</sub> -	H	1.3 ± 0.05	18 ± 2
<b>17</b>	Cyclopropyl	H	Me	-(CH <sub>2</sub> ) <sub>5</sub> -	H	0.9 ± 0.04	11 ± 5
<b>18</b>	Cyclopropyl	H	Cl	-(CH <sub>2</sub> ) <sub>4</sub> -	H	2 ± 1	10 ± 0
<b>19</b>	Cyclopropyl	H	H	-(CH <sub>2</sub> ) <sub>4</sub> -	H	130 ± 10	ND
<b>20</b>	Cyclopropyl	H	H	-(CH <sub>2</sub> ) <sub>4</sub> -	Cl	8 ± 1	1180 ± 78
<b>21</b>	Cyclopropyl	F	Me	-(CH <sub>2</sub> ) <sub>4</sub> -	H	1.2 ± 0.2	18 ± 2
<b>22</b>	H	H	Me	-(CH <sub>2</sub> ) <sub>4</sub> -	H	9 ± 4	73 ± 0
<b>23</b>	Me	H	Me	-(CH <sub>2</sub> ) <sub>4</sub> -	H	12 ± 3	48 ± 10
<b>24</b>	<i>i</i> -Pr	H	Me	-(CH <sub>2</sub> ) <sub>4</sub> -	H	20 ± 5	160 ± 2
<b>25</b>	<i>t</i> Bu	H	Me	-(CH <sub>2</sub> ) <sub>4</sub> -	H	275 ± 104	ND
<b>26</b>		H	Me	-(CH <sub>2</sub> ) <sub>4</sub> -	H	3 ± 1	52 ± 0
<b>27</b>	Cyclobutyl	H	Me	-(CH <sub>2</sub> ) <sub>4</sub> -	H	10 ± 5	50 ± 15
<b>28</b>	Pyridin-2-yl	H	Me	-(CH <sub>2</sub> ) <sub>4</sub> -	H	6 ± 0.5	174 ± 46
<b>29</b>	Isoxazol-3-yl	H	Me	-(CH <sub>2</sub> ) <sub>4</sub> -	H	0.22 ± 0.02	7 ± 2
<b>30</b>	1,2,4-Triazol-3-yl	H	Me	-(CH <sub>2</sub> ) <sub>4</sub> -	H	1166 ± 1	ND

<sup>a</sup> IC<sub>50</sub> values are reported as the mean of at least two experiments.

R<sub>1</sub> are cyclopropyl (**16**, 1.3 nM) and isoxazol-3-yl (**29**, 0.22 nM) which are likely to be of the ideal size to fill the lipophilic binding pocket in this region of the protein (vide infra). Smaller groups do not sufficiently fill the pocket (R<sub>1</sub> = Me, **23**, 12 nM) and larger groups (R<sub>1</sub> = *t*-Bu, **25**, 275 nM) are sterically unfavorable. Even

groups with a slightly larger volume than cyclopropyl, such as isopropyl **24** and cyclobutyl **27**, are about 10-fold less potent than **16** in the enzymatic assay, further indicating the very specific steric requirements in this region as previously observed.<sup>15a</sup> Compound **30** has poor enzymatic potency probably due to the unfavorable placement of a polar triazole moiety into this lipophilic pocket.

The X-ray structure of **16** complexed to p38α was solved and is shown in Figure 4.<sup>21</sup> In the hinge region, hydrogen bonds are made between the carbonyl moiety of the indolin-2-one and both Met109 and Gly110. An additional interaction is seen in this region between the NH of the indolin-2-one and His107 (N–O distance of 3.1 Å). The spiranic cyclopentyl ring sits in an open-ended tunnel and points out towards the solvent – packing interactions are seen with the face of Tyr35 and the side chains of several amino acids including Val30, Leu108, and Gly110. The tolyl amide shows the expected hydrogen-bonding interactions with Asp168 and Glu71 (vide supra). The cyclopropyl group rests in a small lipophilic pocket (vide supra), with close contacts from several amino acids (Glu 71, Leu74, Leu75, Phe169, and Leu171). The methyl group fits into a small groove formed from the sidechains of Ala51, Lys53 and the gatekeeper residue Thr106. A pronounced torsion angle (71°) between the two aromatic rings was observed.

Derivative **16** was extensively profiled as a representative member of this class of indolin-2-one inhibitors. The ADME profile is presented in Table 2. Studies using human hepatic microsomes showed substantial turnover of **16** with both oxidative (hydroxylation of cyclopentyl ring) and NADPH-independent non-oxidative (amide hydrolysis) metabolism occurring (data from MS/MS studies was used to identify the particular metabolites). High metabolic turnover proved to be a general problem with the compounds presented in Table 1 and was ultimately addressed via several strategies.<sup>22</sup> CACO-2 flux data indicated that intestinal permeability should not be a major issue with **16**, although the poor aqueous solubility was a concern (3 µg/mL = ~8 µM).

With regard to early toxicity profiling, compound **16** was found to be moderately cytotoxic in a Chinese hamster ovary (CHO) cell line<sup>23</sup> with an IC<sub>50</sub> = 26 µM and showed 30% hERG block at 10 µM.<sup>24</sup> Compound **16** proved to be reasonably clean in selectivity

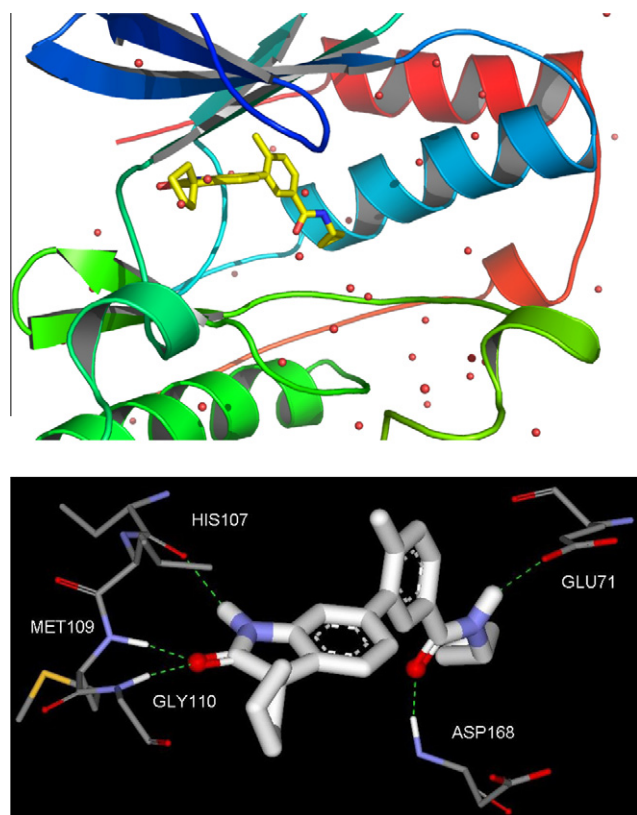


**Figure 4.** Views of the X-ray structure (resolution 2.2 Å) of **16** bound in p38α. H-bonding interactions are shown in the close-up of the active site.

**Table 2**  
ADME Profile for compound for **16**

Parameter	Value
% Turnover in human hepatic microsomes <sup>a</sup>	
+NADPH:	55
-NADPH:	55
CACO2: P <sub>app</sub> (×10 <sup>-6</sup> cm/s) <sup>b</sup> A–B (B–A):	18(10)
Thermodynamic solubility <sup>c</sup> (μg/mL at pH 7.4):	3

<sup>a</sup> % Turnover in human hepatic microsomes using a 30 min incubation period.

<sup>b</sup> Passive permeability through a CACO-2 monolayer determined using 12.5 μM test compound in the presence of 115 nM mannitol.

<sup>c</sup> Twenty-four hour agitation of 0.4 mg test compound in 0.4 mL aqueous buffer at 37 °C followed by filtration and quantification by HPLC–UV.

**Table 3**  
Pharmacokinetic profile of **16** in rat (iv 1 mg/kg)

Terminal t <sub>1/2</sub> (h)	C <sub>max</sub> (ng/mL)	Cl (mL/min/kg)	AUC <sub>0–∞</sub> (ng h/mL)	V <sub>ss</sub> (L/kg)
5.3 <sup>a</sup>	2002	6.6	2532	0.8

<sup>a</sup> Refers to 8% of the dose during the second phase of elimination. Ninety percentage of the dose is eliminated during the 1st phase of elimination with t<sub>1/2</sub> < 1 h.

panels, the most significant findings being the inhibition of 5HT<sub>1B</sub> (87% inhibition at 10 μM) in a panel of 50 receptors (Cerep, France) and the inhibition of human c-Raf (IC<sub>50</sub> = 200 nM) in a panel of 50 kinases (Upstate). No major concern arose when lead compound **16** was tested for inhibition of human cytochromes (IC<sub>50</sub> data: 3A4, 2D6 > 25 μM; 2C19~25 μM; 1A2, 2C9~10 μM).

The iv pharmacokinetic profile of compound **16** in the rat is presented in Table 3. Two elimination phases were seen: an initial elimination phase with a short t<sub>1/2</sub> < 1 h representing >90% of the dose; and a terminal phase with t<sub>1/2</sub> = 5.3 h representing the remainder. Both a low clearance and low volume of distribution were noted. Upon oral dosing at 10 mg/kg low levels of product were detected (C<sub>max</sub> = 367 ng/mL) with a resulting bioavailability of ~10%. Factors such as first pass metabolism (high metabolism in hepatic microsomes ± NADPH) and poor solubility (3 μg/mL at pH 7.4 = ~8 μM) are likely to contribute to the poor oral bioavailability of **16**.

In summary, structure-based design led to a new series of potent and selective indolin-2-one p38α inhibitors. The subsequent optimization of this series will be the subject of further publications.

## References and notes

- Han, J.; Lee, J. D.; Bibbs, L.; Ulevitch, R. J. *Science* **1994**, *265*, 808.
- Raingeaud, J.; Gupta, S.; Rogers, J. S.; Dickens, M.; Han, J.; Ulevitch, R. J.; Davis, R. J. *J. Biol. Chem.* **1996**, *271*, 2886.
- Raingeaud, J.; Whitmarsh, A. J.; Barrett, T.; Derijard, B.; Davis, R. J. *Mol. Cell. Biol.* **1996**, *16*, 1247.
- Badger, A. M.; Bradbeer, J. N.; Votta, B.; Lee, J. C.; Adams, J. L.; Griswold, D. E. *J. Pharmacol. Exp. Ther.* **1996**, *279*, 1453.
- Feldmann, M.; Brennan, F. M.; Maini, R. N. *Annu. Rev. Immunol.* **1996**, *14*, 397.
- Rutgeerts, P.; D'Haens, G.; Targan, S.; Vasilias, E.; Hanauer, S. B.; Present, D. H.; Mayer, L.; van Hogezand, R. A.; Braakman, T.; DeWoody, K. L. *Gastroenterology* **1999**, *117*, 761.
- Foster, M. L.; Halley, F.; Souness, J. E. *Drug News Perspect.* **2000**, *13*, 488.
- Kumar, S.; Boehm, J.; Lee, J. C. *Nat. Rev. Drug Disc.* **2003**, *2*, 717.
- Lee, J. C.; Laydon, J. T.; McDonnell, P. C.; Gallagher, T. F.; Kumar, S.; Green, D.; McNulty, D.; Blumenthal, M. J.; Heyes, J. R.; Landvatter, S. W.; Strickler, J. E.; McLaughlin, M. M.; Siemens, I. R.; Fisher, S. M.; Livi, G. P.; White, J. R.; Adams, J. L.; Young, P. R. *Nature* **1994**, *372*, 739.
- Dominguez, C.; Powers, D. A.; Tamayo, N. *Curr. Opin. Drug Disc. Dev.* **2005**, *8*, 421.
- Ferraccioli, G. F. *Curr. Opin. Anti-Inflammatory Immunomodul. Invest. Drugs* **2000**, *2*, 74.
- Haddad, J. J. *Curr. Opin. Investig. Drugs* **2001**, *2*, 1070.
- Goldstein, D. M.; Kuglstat, A.; Lou, Y.; Soth, M. J. *J. Med. Chem.* **2010**, *53*, 2345.
- Representative patents include: (a) Angell, R. M.; Aston, N. M.; Bamborough, P.; Bamford, M. J.; Cockerill, G. S.; Flack, S. S.; Laine, D. I.; Merrick, S. J.; Smith, K. J.; Walker, A. L. PCT Int. Appl., WO2003032971, **2003**; (c) Almansa, C.; Virgili, M. PCT Int. Appl. WO2007000339, **2007**; (c) Zhang, D.; Tasker, A.; Sham, K. K. C.; Chakrabarti, P. P.; Falsey, R. J.; Herberich, B. J.; Pettus, L. H.; Rzasza, R. M. PCT Int. Appl. WO2008045393, **2008**; (d) Vidal, B.; Eastwood, P. R.; Gonzalez, J.; Esteve, C. PCT Int. Appl. WO2008107125, **2008**.
- (a) Angell, R.; Aston, N. M.; Bamborough, P.; Buckton, J. B.; Cockerill, S.; de Boeck, S. J.; Edwards, C. D.; Holmes, D. S.; Jones, K. L.; Laine, D. I.; Patel, S.; Smees, P. A.; Smith, K. J.; Somers, D. O.; Walker, A. L. *Bioorg. Med. Chem. Lett.* **2008**, *18*, 4428; (b) Angell, R. M.; Angell, T. D.; Bamborough, P.; Bamford, M. J.; Chung, C.; Cockerill, S. G.; Flack, S. S.; Jones, K. L.; Laine, D. I.; Longstaff, T.; Ludbrook, S.; Pearson, R.; Smith, K. J.; Smees, P. A.; Somers, D. O.; Walker, A. L. *Bioorg. Med. Chem. Lett.* **2008**, *18*, 4433.
- Wroblewski, S. T.; Lin, S.; Hynes, J.; Wu, H.; Pitt, S.; Shen, D. R.; Zhang, R.; Gillooly, K. M.; Shuster, D. J.; McIntyre, K. W.; Doweiko, A. M.; Kish, K. F.; Tredup, J. A.; Duke, G. J.; Sack, J. S.; McKinnon, M.; Dodd, J.; Barrish, J. C.; Schieven, G. L.; Leftheris, K. *Bioorg. Med. Chem. Lett.* **2008**, *18*, 2739; (b) Hynes, J., Jr.; Dyckman, A. J.; Lin, S.; Wroblewski, S. T.; Hong, W.; Gillooly, K. M.; Kanner, S. B.; Lonial, H.; Loo, D.; McIntyre, K. W.; Pitt, S.; Shen, D. R.; Shuster, D. J.; Yang, X.; Zhang, R.; Behnia, K.; Zhang, H.; Marathe, P. H.; Doweiko, A. M.; Tokarski, J. S.; Sack, J. S.; Pokross, M.; Kiefer, S. E.; Newitt, J. A.; Barrish, J. C.; Dodd, J.; Schieven, G. L.; Leftheris, K. *J. Med. Chem.* **2008**, *51*, 4.
- For further discussion on the 'flip' binding mode of unrelated series see: (a) Fitzgerald, C. E.; Patel, S. B.; Becker, J. W.; Cameron, P. M.; Zaller, D.; Pikounis, V. B.; O'Keefe, S. J.; Scapin, G. *Nat. Struct. Biol.* **2003**, *10*, 764; (b) Natarajan, S. R.; Heller, S. T.; Nam, K.; Singh, S. B.; Scapin, G.; Patel, S.; Thompson, J. E.; Fitzgerald, C. E.; O'Keefe, S. J. *Bioorg. Med. Chem. Lett.* **2006**, *16*, 5809.
- Kende, A. S.; Hodges, J. C. *Synth. Commun.* **1982**, *12*, 1.
- (a) Robertson, D. W.; Krushinski, J. H.; Pollock, G. D.; Wilson, H.; Kauffman, R. F.; Hayes, J. S. *J. Med. Chem.* **1987**, *30*, 824; (b) Di, M. A.; Foulon, L.; Garcia, G.; Nisato, D.; Roux, R.; Serradeil-Legal, C.; Valette, G.; Wagnon, J. Eur. Pat. Appl., EP636608, **1995**.
- For full details of the biological assays used in this publication see: Lumeras, W.; Caturla, F.; Vidal, L.; Esteve, C.; Balagué, C.; Orellana, A.; Dominguez, M.; Roca, R.; Huerta, J. M.; Godessart, N.; Vidal, B. *J. Med. Chem.* **2009**, *52*, 5531.
- Coordinates and structure factors for the complex of p38α with **16** have been deposited in the RCSB Protein Data Bank (access code 3RIN).
- Eastwood, P. et al., unpublished results.
- Cytotoxicity assay*: Trypsinized CHO cells (10,000 cells/well) were incubated in 96-well plates in a culture medium for 24 h at 37 °C with 5% CO<sub>2</sub>. The culture medium was removed and the plates washed with dPBS (Biowhittaker BE-17-512F or Sigma D8537). Hundred microliters of culture medium containing the test compounds was added to the plate wells and incubation was continued for 24 h. The cells were then washed with 100 μL of dPBS and the reduction of the ATP-status of the cells was studied with ATPLite, a luminescence ATP detection assay system (PerkinElmer, ref: 6016941). The luminescence was measured using a Luminoskan luminometer (ThermoElectron). To create a standard curve luminescence values versus cell number were plotted and the data was adjusted to a lineal equation. Luminescence values of the samples were interpolated to obtain cell count. The inhibition of the ATP status for each test compound was determined by using at least eight different concentrations ran in duplicate. IC<sub>50</sub> values (test compound concentration at which the cell number is reduced to half) were obtained by non-linear regression using XLfit4.0 software.
- Crumb, W. J.; Cavero, I. *Current Protocols in Pharmacology* **2003**, Online ISBN: 9780471141754, 10.8.1–10.8.18.